Pharmaceutical Research, Vol. 22, No. 6, June 2005 (© 2005)
DOI: 10.1007/s11095-005-4595-y

Research Paper

Solid-State Fluorescence Studies of Some Polymorphs of Diflunisal*

Harry G. Brittain,[1,3] Bruce J. Elder,[2] Paul K. Isbester,[2] and Allen H. Salerno[2]

Received December 20, 2004; accepted March 7, 2005

Purpose. The solid-state luminescence spectroscopy of organic molecules is strongly affected by the effects of excited state energy transfer, with the fluorescence of solids often differing significantly from the fluorescence of the molecule dissolved in a solution phase. Because the magnitude of these solid-state effects is determined by the crystallography of the system, solid-state fluorescence studies can be used to gain insight into the polymorphism of the system. To this end, the spectroscopic properties of four polymorphs of diflunisal have been obtained, and compared to the properties of the molecule in the solution phase.
Methods. Fluorescence excitation and emission spectra were obtained on four polymorphic forms of diflunisal, and on the compound dissolved in water.
Results. It was found that exciton effects dominate the excitation spectra of diflunisal in the four studied polymorphic forms. These phenomena lead to a decrease in the energy of the excitation bands relative to that observed for the free molecule in fluid solution, and in a splitting of the excitation peak into two Davydov components.
Conclusions. The trends in the excitation and emission spectra led to the grouping of diflunisal Forms I, II, and III into one category, and diflunisal Form IV into a separate category. Because other work has established that Form IV is characterized by the highest crystal density and consequent degree of intermolecular interaction, the magnitude of the exciton coupling can be used to estimate the degree of face-to-face overlap of the salicylate-type fluorophores.

KEY WORDS: diflunisal; exciton splitting; fluorescence spectroscopy; polymorphism; X-ray powder diffraction.

INTRODUCTION

Once the existence of polymorphism or solvatomorphism is established for a given compound by means of a crystallographic technique, there is no doubt that solid-state spectroscopy can play a vitally important role in the study of that system (1–4). For instance, if the modes of group vibrations are affected by the structural differences inherent to the various crystal forms, then solid-state vibrational spectroscopy (either infrared absorption (5) or Raman scattering (6,7)) can be used to deduce information specific to the functional group affected by the differing crystallography. Similarly, when the magnetic environments of nuclei are perturbed by structural differences arising from different crystal structures, then study of the chemical shifts within solid-state nuclear magnetic resonance spectra can yield important structural details of the system (8–10).

Perhaps less well recognized is that when the differing crystal structures of polymorphs or solvatomorphs cause an alteration of molecular orbital energies, then analytical techniques that measure transitions among the electronic states derived from these orbitals can be used to obtain additional information on the systems. The numerous observations recorded in the literature that different polymorphs of certain molecules can be characterized by the existence of different colors (11–13) represents one application of reflectance spectroscopy in the visible region of the spectrum. Because fluorescence spectroscopy is derived from transitions among the same electronic states (14), then it is to be anticipated that the excitation and emission spectra of luminescent molecules could be used to study the patterns of energy flow within the respective solids. Such methodology was recently used to deduce kinetic information associated with the phase transformation of carbamazepine anhydrate Form III to its dihydrate phase (15).

Diflunisal can be envisioned of as consisting of a difluorobenzene group that has been linked to a salicylic acid group:

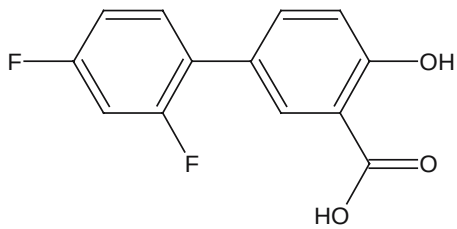

* This paper is to be considered as Part 2 in the series, "Studies of the Fluorescence of Pharmaceutical Materials in the Solid State," with reference (15) being the preceding paper in the series.

[1] Center for Pharmaceutical Physics, Milford, New Jersey, USA.
[2] Albany Molecular Research, Albany, New York, USA.
[3] To whom correspondence should be addressed. (e-mail: hbrittain@earthlink.net)

It is now well established that diflunisal is capable of being obtained in a number of polymorphic and solvatomorphic forms, although ambiguity exists regarding the nomenclature of these (16–21). Because the molecule contains a salicylate group (well known to fluoresce in both its solution and solid phases), it was anticipated that diflunisal would also be fluorescent both in the solution phase and in the various crystal forms. In the present work, solid-state fluorescence spectroscopy has been used to study the effects on the electronic structure of diflunisal that were induced by the structural differences existing in four crystal forms.

MATERIALS AND METHODS

The crystal form identification used in this work follows that of Martinez-Oharriz *et al.* (17). Bulk diflunisal substance was obtained from Sigma, where this commercial product was obtained as crystal Form-II. The other three polymorphs were crystallized according to the literature procedure (17), where an adequate amount of the drug substance was dissolved in either chloroform (to prepare Form I), ethanol (to prepare Form III), or toluene (to prepare Form-IV) at 60°C, and then rapidly cooled to 6°C in a refrigerator. The polymorphic identity of the isolated crystal forms was confirmed using X-ray powder diffraction.

X-ray powder diffraction (XRPD) patterns were obtained using a Rigaku MiniFlex powder diffraction system, equipped with a horizontal goniometer in the θ/2θ mode. The X-ray source was nickel-filtered K-α emission of copper (1.55314 Å). Samples were packed into an aluminum holder using a back-fill procedure, and were scanned over the range of 6 to 48 degrees 2θ, at a scan rate of 0.5 degrees 2θ/min. Using a data acquisition rate of 1 point per second, the scanning parameters equate to a step size of 0.0084 degrees 2θ. Calibration of each powder pattern was effected using the characteristic scattering peaks of aluminum at 44.738 and 38.472 degrees 2θ, so the useful range for sample characterization range was 6 to 36 degrees 2θ.

The UV/VIS absorption spectrum of diflunisal in water was obtained using a Perkin–Elmer model Lambda 3B spectrophotometer. The spectrum was solvent-corrected, and obtained on a 13.2 μg/ml solution.

All solution-phase and solid-state fluorescence excitation and emission spectra were obtained on samples packed into 5-mm glass NMR tubes. Preliminary spectra were obtained on a Perkin–Elmer LS 5B luminescence spectrometer to delineate spectroscopic areas of interest, and to establish the relative intensities of the various spectra. The liquid cell holder of the spectrometer was removed, and replaced by an aluminum block having a hole drilled through its length to facilitate kinematic placement of the sample tube. The block had an additional lateral removal of metal that permitted irradiation of the sample and detection of fluorescence at right-angles.

High-resolution excitation spectra of the solid samples were subsequently obtained on a spectrometer specially constructed for this purpose. Sample excitation was effected by using a 0.5 meter monochromator (Spex model 1870) to discriminate the output of a 300 watt xenon arc lamp. The grating used in this device was blazed at 300 nm, ruled at 1200 g/mm, and the monochromator was characterized by a dispersion of 1.2 nm/mm slit width. The input and output slits were set at 0.5 mm, setting the resolution of the spectra at 0.6 nm, and so the reported wavelength values were all rounded to the nearest 0.5 nm. The fluorescence was allowed to pass through a long-pass filter (1% w/v solution of sodium nitrite in a 1 cm cell) to remove scattering light, and then detected by an end-on photomultiplier tube (Thorn EMI type 6256QB having S-11 response). After current-to-voltage conversion, the spectra were electronically acquired using a data acquisition rate of 1 point per second.

High-resolution emission spectra of the solid samples were obtained on a separate spectrometer specially dedicated for this purpose. Sample excitation was effected by using a combination of glass and solution filters (22) to isolate the desired output of a 250 watt xenon arc lamp. The sample was irradiated using front-face excitation, and the fluorescence analyzed by a 0.5 meter monochromator (Spex model 1870) having a grating blazed at 500 nm and ruled at 1200 g/mm. The dispersion of this monochromator was 1.2 nm/mm slit width, so with the input and output slits set at 0.5 mm, the resolution of the spectra was 0.8 nm and the reported wavelength values were therefore all rounded to the nearest 0.5 nm. The fluorescence was detected by an end-on photomultiplier tube (Thorn EMI type 9558QB having S-20 response), and after current-to-voltage conversion, the spectra were electronically acquired using a data acquisition rate of 1 point per second.

RESULTS

Solution Phase Studies

The absorption and fluorescence spectroscopies of diflunisal were first studied in the solution phase in order to

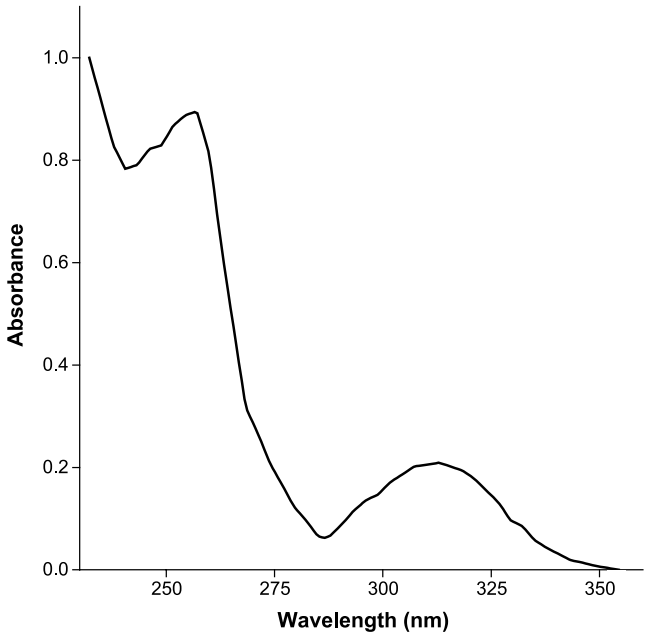

Fig. 1. Ultraviolet absorption spectrum of a 13.2 μg/mL solution of diflunisal in water.

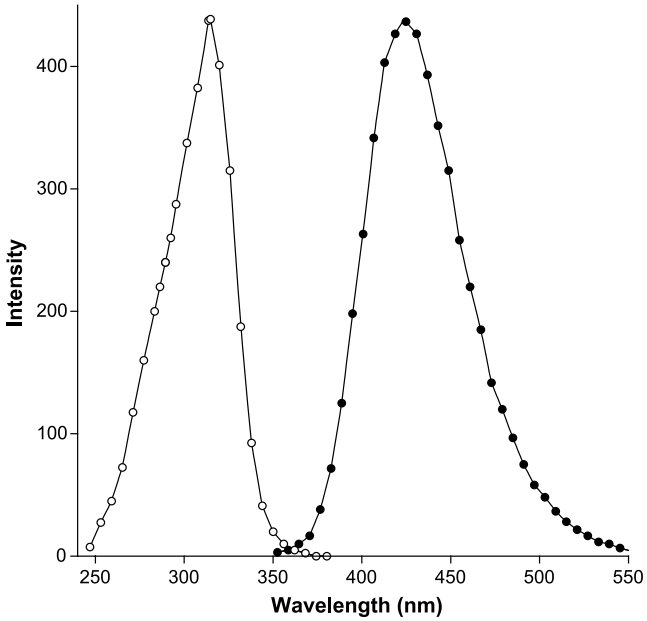

Fig. 2. Solution phase excitation (O) and emission (●) spectra of a 13.2 μg/mL solution of diflunisal in water.

better understand the basic spectroscopy involved. The absorption spectrum of a 13.2 μg/ml solution of diflunisal in water is shown in Fig. 1 and consists of two absorption maxima. Given the free rotation that would exist in the solution phase about the bond connecting these two groups, it is likely that the energy states associated with each aromatic ring would be decoupled from each other and be separately observed in the absorption spectrum. Thus, the band observed at 257 nm is most likely due to absorbance associated with the difluorobenzene group, and the band observed at 313 nm would then be associated with absorbance in the salicylate group.

The solution phase excitation and emission spectra of the 13.2 μg/mL solution of diflunisal in water are shown in Fig. 2. It was found that excitation into the difluorobenzene group did not lead to measurable fluorescence, but that excitation into the salicylate group (wavelength of 314 nm) led to fluorescence having a wavelength maximum at 424 nm.

Solid-State Studies

The X-ray powder diffraction patterns of the four polymorphs of diflunisal are shown in Fig. 3. The nomenclature used here to identify the various crystal forms is that given in (17), which may be summarized as follows:

Form I	Rapid cooling from chloroform
Form II	Antisolvent of water to ethanol solution
Form III	Rapid cooling from ethanol
Form IV	Rapid cooling from toluene

Confusion exists in the literature regarding the nomenclature and identity of the polymorphic forms of diflunisal, but a comparison of the powder patterns of Fig. 3 with the powder diffraction data published by Bauer-Brandl *et al.* (20) yields the following correlation:

Crystal form identification used in the current work	Crystal form identification used by Bauer-Brandl (20)
Form I	Modification D
Form II	Modification B
Form III	Modification C
Form IV	Modification A

The excitation and emission spectra of diflunisal Form I are shown in Fig. 4. The excitation spectrum (emission analyzing wavelength of 430 nm) was found to consist of two semi-resolved bands, with the most intense peak being located at a wavelength of 345.5 nm and the shoulder at approximately 379 nm. As will be noted for the other solid-state polymorphic forms, the non-equivalence of the solid-state and solution phase excitation maxima indicates the existence of cooperative phenomena in the solid state. Excitation into each of these bands yielded equivalent fluorescence spectra, characterized by emission maxima at 424.0 nm and 425.0 nm, respectively. The maxima of these emission bands are effectively equivalent to the maximum of the emission band measured from the solution phase investigation.

The excitation and emission spectra obtained for diflunisal Form II are shown in Fig. 5. The maxima of the two peaks in the excitation spectrum (emission analyzing wavelength of 430 nm) could now be identified, with the most intense wavelength maximum being observed at 343.0 nm and the second peak at 379.5 nm. As was observed for Form I, neither excitation wavelength maximum corresponded to the wavelength of the excitation maximum of diflunisal in the solution phase, continuing to indicate the existence of cooperative excitation phenomena in the solid state. Excitation into each of these bands yielded equivalent fluorescence spectra, characterized by emission maxima at 424.5 nm and 424.0 nm, respectively. The maxima of these emission bands are not significantly different from the maximum of the emission band measured during the solution phase investigation.

The excitation and emission spectra of diflunisal Form III are shown in Fig. 6, and feature an even better degree of resolution between the two bands of the excitation spectrum. The excitation maxima (emission analyzing wavelength of 430 nm) were observed at 345.0 nm and 379.5 nm. As was observed for Forms I and II, the non-equivalence of the solid-state and solution phase excitation maxima indicates the existence of cooperative excitation phenomena in the solid state. Excitation into each of these bands yielded fluorescence spectra characterized by emission maxima at 425.0 nm and 425.5 nm, respectively. The maxima of these emission bands are not significantly different from the maximum of the emission band measured during the solution phase investigation.

The excitation and emission spectra that were obtained for diflunisal Form-IV are shown in Fig. 7. The excitation spectrum (obtained at an emission analyzing wavelength of 460 nm) exhibited the highest resolution of the two excitation bands, with the first being observed at 343.5 nm and the second at 393.0 nm. Excitation into each of these bands yielded equivalent fluorescence spectra, both of which were characterized by emission maxima at 454.0 nm. The maxima

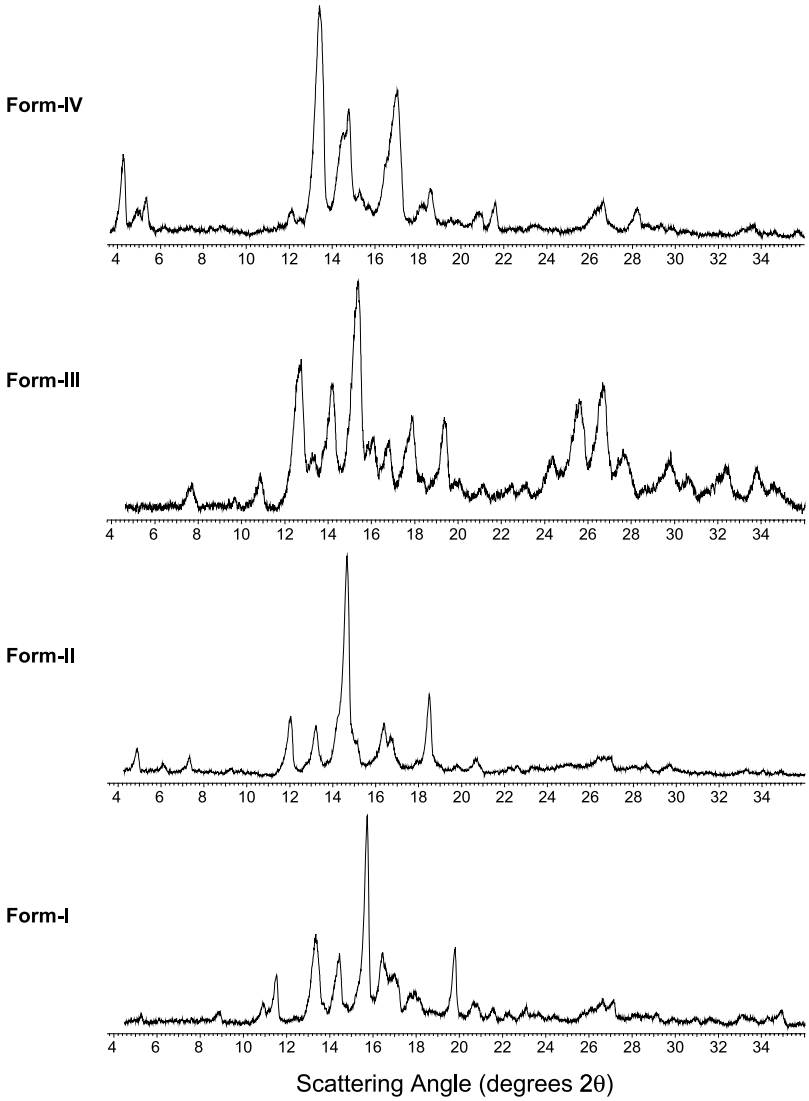

Fig. 3. X-ray powder diffraction patterns of the four polymorphs of diflunisal.

of these emission bands is significantly shifted to lower energies relative to the maximum of the emission band measured during the solution phase investigation.

The overall fluorescence intensities of the four polymorphs of diflunisal were significantly reduced relative to the intensity of the molecule in the solution phase, undoubtedly reflecting the effects of solid-state energy transfer processes. The fluorescence intensities of the solid-state polymorphs followed the general order of Form IV ≈ Form III > Form II > Form I.

DISCUSSION

Solution Phase Studies

An understanding of the spectroscopy of a molecule in its crystalline state can be greatly aided by an understanding of the spectroscopy of the isolated molecule unperturbed by the effects of energy transfer. In the absence of spectroscopy conducted in the gas phase, the next best model is represented by the molecule in a condensed amorphous state, such as would exist in a fluid solution. Under such circumstances, the ground state of the molecule can be described as an electronic wave function onto which is superimposed a sequence of vibrational wave functions. This has been illustrated in Fig. 8 by horizontal levels proper to each curve (rotational states have not been included for the sake of clarity in the figure).

A molecule in thermal equilibrium at ambient temperature will exist largely in the lowest vibrational state of its ground state (i.e., the v = 0 level of state S_0). Absorption of light causes excitation of the molecule into its excited state, and according to the Franck–Condon principle the most intense vibrational component of the transition will be the one that takes place at the same configuration of the ground state (drawn as the v = 3 level of state S_1). This, of course, places the molecule into an excited vibrational level of the excited state, which then rapidly decays into the lowest vibrational state of the excited state (i.e., the v = 0 level of state S_1). Fluorescence will take place out of the lowest vibrational level of the excited state, but now with the most intense transition being the one that takes place at the same configuration of the excited state (drawn as the v = 2 level of state S_0).

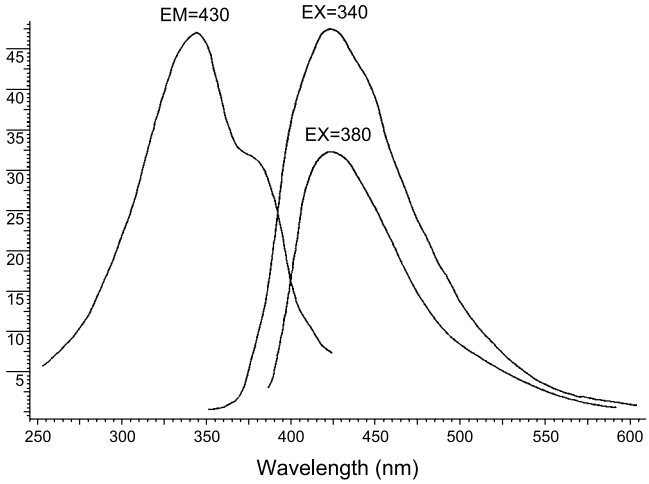

Fig. 4. Excitation spectrum of diflunisal Form I obtained at an emission wavelength of 430 nm, and emission spectra obtained at excitation wavelengths of 340 nm and 380 nm. The intensity scale is in arbitrary units, but has been scaled so as to facilitate comparison with the intensity scales of Figs. 5–7.

Although it is usual practice to identify the energies of spectroscopic transitions by the positions of their peak maxima, those peak energies do not correspond to the difference in the pure electronic energies of the two states. In other words, the maximum of the excitation spectrum for the molecule in Fig. 8 would correspond to the vibronic $S_0(v = 0) \rightarrow S_1(v = 3)$ transition, while the maximum in the emission spectrum would correspond to the vibronic $S_1(v = 0) \rightarrow S_0(v = 2)$ transition. However, it is the energy difference between the $S_0(v = 0)$ and the $S_1(v = 0)$ states that represents the energy difference between the pure electronic states, and the value of this parameter can be taken as approximating the energy separation of the free molecule.

From an consideration of Fig. 8, it is clear that the energy of the $S_0(v = 0) \rightarrow S_1(v = 0)$ excitation transition must be exactly the same as the energy of the $S_1(v = 0) \rightarrow S_0(v = 0)$ emission transition. Furthermore, the $S_0(v = 0) \rightarrow S_1(v = 0)$ excitation would be observed at the lowest energy (i.e., at the longest wavelength) of the excitation band system, and the $S_1(v = 0) \rightarrow S_0(v = 0)$ emission would be observed at the highest energy (i.e., at the shortest wavelength) of the emission band system. In the absence of resolved vibronic bands in the spectra, this energy is most commonly estimated from knowledge of the wavelength where the excitation and emission curves intersect. For the diflunisal solution-phase spectra of Fig. 2, this intersection is found to be 361 nm, which is equivalent to an energy of 27,700 cm^{-1}.

With the assignment of the energy of the $S_1(v = 0) \rightarrow S_0(v = 0)$ transition as 27,700 cm^{-1}, one may calculate the amount of vibrational energy that must be dissipated in the excitation process to enable the molecule to decay down to the $S_1(v = 0)$ state. The peak maximum in the excitation spectrum (observed at 314 nm, or 31,850 cm^{-1}) corresponds to the most favorable Franck–Condon transition, with the energy of this $S_1(v = i)$ state being 4510 cm^{-1} greater than the energy of the $S_1(v = 0)$ state. This energy would be dissipated either by a cascade through several vibrational levels of a single mode of the excited state, or through a combination of excited state modes.

Solid-State Studies

The solid-state spectroscopy of diflunisal in each of its different polymorphic forms facilitates a classification into two types:

Type A (Forms I, II, and III): The two excitation bands are located at approximately 345 nm and 380 nm, both of which are shifted to lower energies relative to the excitation band of the solution phase molecule (314 nm). The maxima observed in each of the fluorescence spectra are located at approximately 425 nm, which is not significantly different from that of diflunisal in the solution phase (424 nm).

Type-B (Form IV): The two excitation bands are located at approximately 345 nm and 395 nm, a greater degree of separation than noted for the Type A polymorphs, and both of which are shifted to lower energies relative to the excitation band of the solution phase molecule (314 nm). The maxima observed in each of the fluorescence spectra are located at approximately 455 nm, which is significantly shifted to lower energies relative to that of diflunisal in the solution phase (424 nm).

This classification enables one to conclude that two types of phenomena are operational in the diflunisal crystal systems. The first of these is a physical state effect, manifested in the shift to lower energy observed for the excitation energies of all solid-state diflunisal forms relative to the solution phase energy. The second of these is a polymorphism effect, which is manifested in spectroscopic differences among the polymorphs and which culminates in the Type A and Type B classification schemes.

The same type of spectroscopic sorting just described was also derived on the basis of solid-state infrared spectroscopic studies of the diflunisal polymorphs that were published elsewhere (20). In that work, modifications B, C, and D (which are the same as Forms II, III, and I, respectively) could be grouped in a different class from modification A (which is the same as Form IV) on the basis

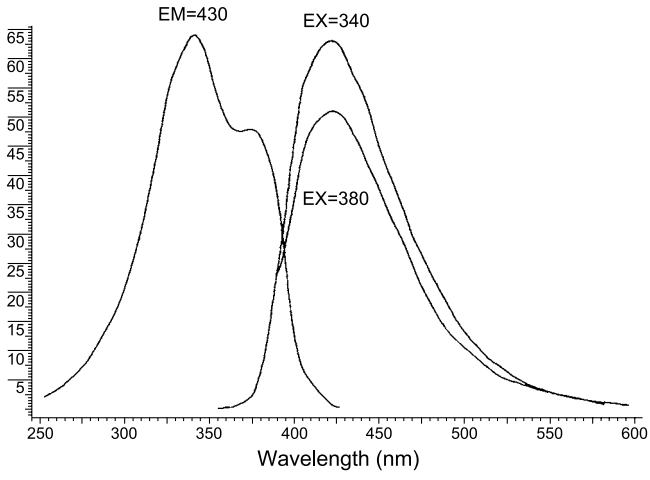

Fig. 5. Excitation spectrum of diflunisal Form II obtained at an emission wavelength of 430 nm, and emission spectra obtained at excitation wavelengths of 340 nm and 380 nm. The intensity scale is in arbitrary units, but has been scaled so as to facilitate comparison with the intensity scales of Figs. 4, 6, and 7.

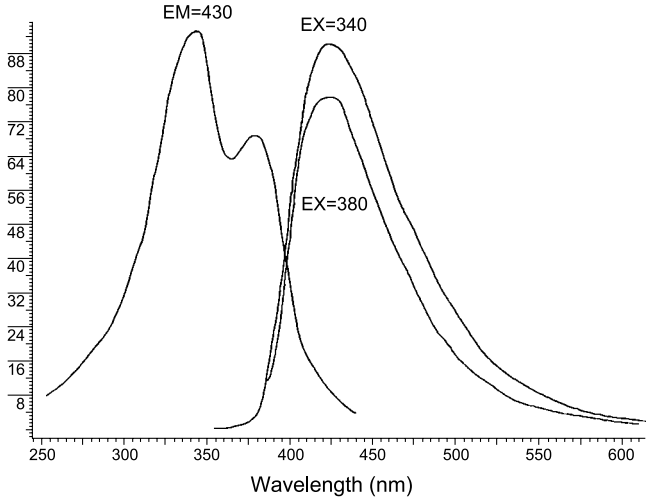

Fig. 6. Excitation spectrum of diflunisal Form III obtained at an emission wavelength of 430 nm, and emission spectra obtained at excitation wavelengths of 340 nm and 380 nm. The intensity scale is in arbitrary units, but has been scaled so as to facilitate comparison with the intensity scales of Figs. 4, 5, and 7.

of the frequencies associated with carbonyl bands, O-H stretching modes, and C-F stretching vibrations.

The repetitive three-dimensional structure of each of the solid-state form of diflunisal locks the component molecules in well-defined orientations with respect to each other. As a result, energy transfer between molecules, via the common radiation field, is often facilitated, and such radiationless transfer of energy can take place over appreciable distances in the crystal. In the absence of interactions between molecules in a crystal, one would anticipate that the sequence of energy levels existing in the solution phase would be largely preserved in the solid state. However, although the ground electronic state is localized on individualized molecules even in the crystalline state, the excited electronic states of these can be so strongly interactive that excitation energy becomes delocalized among the coupled molecules. Frenkel first termed such a delocalized excited state an exciton (23), and the theory of excitons has been thoroughly applied to organic crystals by Davydov (24).

Craig and Walmsley (25) have summarized a number of characteristics pertaining to molecular excitons. Since the transfer of electronic energy between the excited molecules is rapid relative to the time frame of fluorescence, the delocalization of excitation energy has the effect of extending the excited state molecular orbital over the ensemble of molecules involved in the energy transfer. For a pair of molecules, the interaction leads to a splitting of the single-molecule energy level into a pair of levels, where the magnitude of the splitting is determined by the strength of the coupling. This type of splitting is commonly referred to as Davydov splitting, and becomes manifest in the appearance of new bands in the excitation spectrum. In addition, the theory predicts that the mean frequency of the Davydov components would be displaced to lower energies from that of the free molecule value as a result of cooperative interactions in the crystalline state.

For an ensemble of *N* identical, decoupled, molecules, the wave functions (ϕ_i) of the excited states where one molecule is excited and the others are in the ground state can be written as:

$$\phi_1 = \psi^*(1)\psi(2)\psi(3)\cdots\psi(n)$$
$$\phi_2 = \psi(1)\psi^*(2)\psi(3)\cdots\psi(n)$$
$$\phi_3 = \psi(1)\psi(2)\psi^*(3)\cdots\psi(n)$$
$$\cdots\cdots\cdots\cdots\cdots\cdots$$
$$\phi_N = \psi(1)\psi(2)\psi(3)\cdots\psi^*(n)$$

where $\psi(i)$ is the wave function of the molecule it its ground state and $\psi^*(j)$ is that of a molecule in the excited state. If there is no interaction between the molecules, then all of the excited state wave functions will have the same energy. But if transfer of excitation energy between the excited states takes place, then those states are not stationary states of the system and must be mixed. The mixing process yields a new series of states (Ψn) that will be formed as linear combinations of the ϕ_i functions, and which will differ from each other by the values of the coefficients, C_{nm}:

$$\Psi_1 = C_{11}\phi_1 C_{12}\phi_2 C_{13}\phi_3\cdots C_{1m}\phi_N$$
$$\Psi_2 = C_{21}\phi_1 C_{22}\phi_2 C_{23}\phi_3\cdots C_{2m}\phi_N$$
$$\Psi_3 = C_{31}\phi_1 C_{32}\phi_2 C_{33}\phi_3\cdots C_{3m}\phi_N$$
$$\cdots\cdots\cdots\cdots\cdots\cdots$$
$$\Psi_N = C_{n1}\phi_1 C_{n2}\phi_2 C_{n3}\phi_3\cdots C_{nm}\phi_N$$

As illustrated in Fig. 9, the result of exciton coupling is to produce an excitation multiplet corresponding to a band of n levels, each differing in energy by small amounts. The overall spread of the excitation band is determined by the strength of the coupling, and one can actually observe a separation between the symmetric linear combinations and the anti-symmetric linear combinations if the coupling is sufficiently strong. More detailed mathematical treatments of exciton coupling and splitting are available in the literature (24–26).

In molecular crystals, the magnitude of the interaction energy and degree of exciton coupling would necessarily be

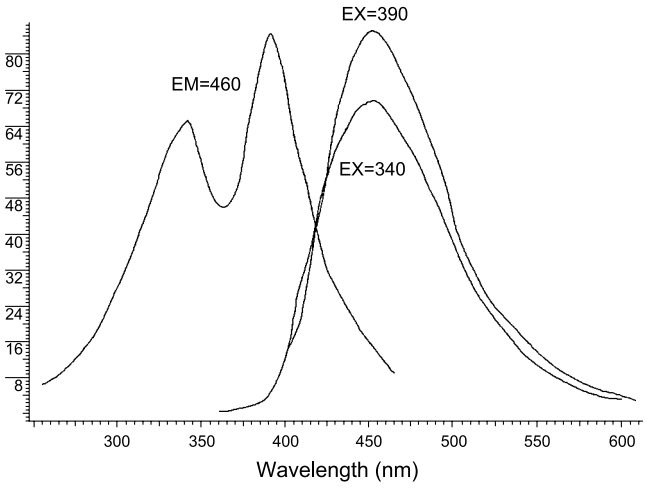

Fig. 7. Excitation spectrum of diflunisal Form IV obtained at an emission wavelength of 460 nm, and emission spectra obtained at excitation wavelengths of 340 nm and 390 nm. The intensity scale is in arbitrary units, but has been scaled so as to facilitate comparison with the intensity scales of Figs. 4–6.

dependent on the relative orientation of the molecules in the crystal, as well as on their distance separation. It follows that since polymorphic crystal forms are characterized by the existence of differing structural properties, the nature of the exciton coupling in the various forms would be dictated by the particular structural characteristics of each form. As a result, one would anticipate that the magnitude of the Davydov splitting, and the degree of shifting of the levels, would be dependent on the exact structural details existing in the different polymorphic forms.

As discussed above and illustrated in Figs. 4–7, the excitation spectrum of each diflunisal polymorph was observed to consist of two peaks, and the energy difference between these can be taken as defining the magnitude of the Davydov splitting. The three polymorphs exhibiting the Type A behavior exhibited excitation peaks at approximately 28,985 cm^{-1} and 26,315 cm^{-1}, for a Davydov splitting of 2670 cm^{-1}. One can then calculate the energy of this excited state in the absence of excited state delocalization as the average of the energies of the Davydov components. This energy is found to be 27,650 cm^{-1}, a value that is extremely close to the calculated energy of 27,700 cm^{-1} for the solution phase $S_1(v = 0)$ state. This equivalence in excited state energy, and the fact that the Type A fluorescence is effectively equivalent in energy to the solution phase fluorescence, leads to the conclusion that the electronic states of the Type A diflunisal forms are not significantly different from those of the solution phase molecule, with the exception of the Davydov splitting caused by the delocalization of energy upon excitation.

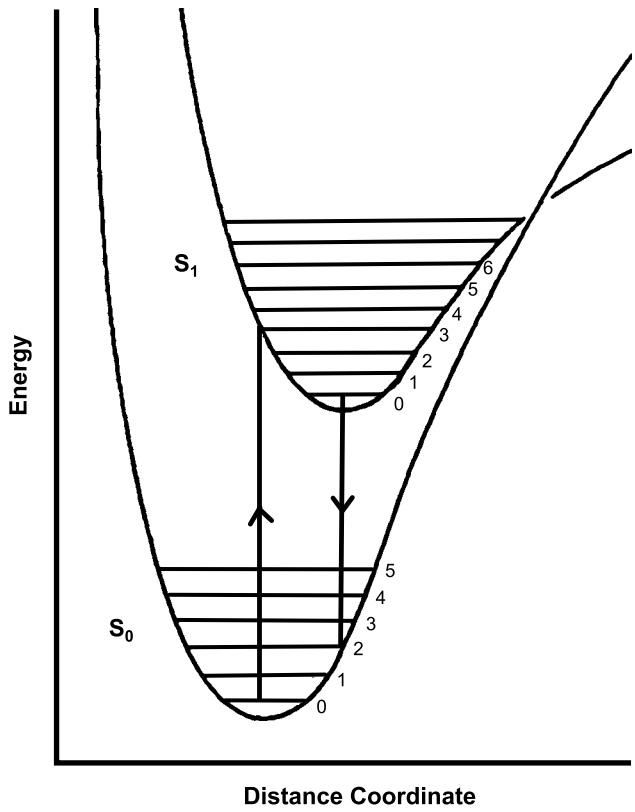

Fig. 8. Schematic energy level diagram of the ground and first excited state of a fluorescent organic molecule. The vertical lines correspond to the transitions characterized by the most favorable Franck–Condon overlap.

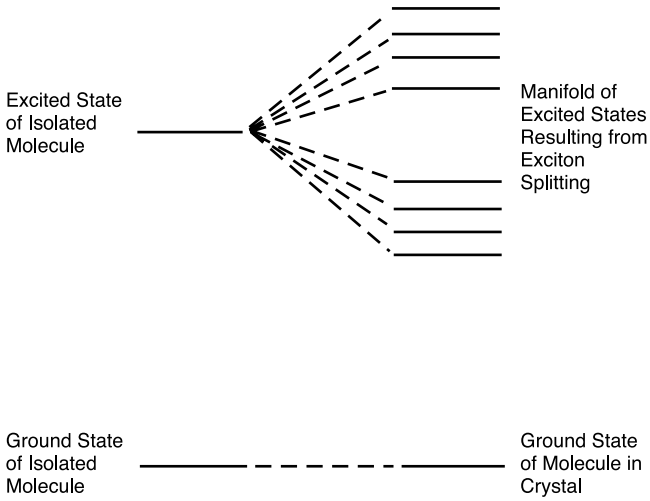

Fig. 9. Schematic energy level diagram illustrating the effect of exciton coupling that results in a splitting of the excited state into a manifold of states.

On the other hand, diflunisal Form IV exhibited the very different pattern of spectroscopic behavior denoted as Type B. Here, the energies of the excitation peaks were approximately 28,985 cm^{-1} and 25,315 cm^{-1}, for a Davydov splitting of 3670 cm^{-1}. The average of the Davydov components is found to be 27,150 cm^{-1}, making the energy of the unsplit state not equivalent to the calculated energy of 27,700 cm^{-1} for the solution phase $S_1(v = 0)$ state. Considering with the fact that the Type B fluorescence is substantially shifted to lower energy relative to that of the solution phase fluorescence, one concludes that the electronic states of the Type B diflunisal form are significantly different from those of the solution phase molecule.

The conclusions drawn from the spectroscopic studies indicate a fundamental difference in the electronic states of the Type A and Type B forms that must have its origins in the crystallographic differences between the different polymorphs. As discussed above, the magnitude of the interaction energy in molecular organic crystals is dependent on the relative orientation of the molecules in the solid as well as on their distance separation. This interaction can be particularly strong for aromatic-type systems such as anthracene, when the molecular planes are coplanar to each other, and the energy transfer mechanism depends on the degree of face-to-face overlap of the aromatic rings (24).

Although the structures of the four anhydrous diflunisal polymorphs have not yet been determined by means of single-crystal diffraction, the powder diffraction of modifications A through D (and hence Forms I through IV) have been indexed and lattice parameters reported (20). Most importantly, it has been reported in this work that the molecular volume of diflunisal in the unit cell is lowest for modification A (i.e., Form IV), and consequently the packing of molecules in this form must be extremely dense relative to the other forms. It was also concluded that the molecules in this form do not form dimers.

Because the magnitude of the exciton phenomena in the various diflunisal polymorphs must be a direct consequence

of the crystal structure defining such phenomena, and since the fluorescence processes are undoubtedly associated with the salicylate moiety, it is reasonable conclude that the different polymorphs differ in the degree of face-to-face interactions between salicylate groups in the differing structures. With the propensity of diflunisal in Forms I, II, and III to form dimers, and the apparent inability of Form IV to form such structures, one must conclude that there must be a degree of overlap of salicylate groups in Form IV that is substantially greater than the degree of overlap in the other polymorphic forms.

CONCLUSIONS

It has been found that exciton effects dominate the excitation spectra of diflunisal in the four studied polymorphic forms. These phenomena lead to a decrease in the energy of the excitation bands relative to that observed for the free molecule in fluid solution, and in a splitting of the excitation peak into two Davydov components. The trends in the excitation and emission spectra led to the grouping of diflunisal Forms I, II, and III into one category, and diflunisal Form IV into a separate category. Since other work has established that Form IV is characterized by the highest crystal density and consequent degree of intermolecular interaction, the magnitude of the exciton coupling can be correlated the degree of face-to-face overlap of the fluorescent salicylate fluorophores.

REFERENCES

1. T. L. Threlfall. Analysis of organic polymorphs—a review. *Analyst* **120**:2435–2460 (1995).
2. H. G. Brittain. Spectral methods for the characterization of polymorphs and solvates. *J. Pharm. Sci.* **86**:405–412 (1997).
3. H. G. Brittain. Methods for the characterization of polymorphs and solvates. In H.G. Brittain (ed.), *Polymorphism in Pharmaceutical Solids*, Marcel Dekker, New York, 1999, Chap. 6, pp. 227–278.
4. J. Bernstein. Analytical techniques for studying and characterizing polymorphs. *Polymorphism in Molecular Crystals*, Clarendon Press, London, 2002, Chap. 4, pp. 94–150.
5. D. E. Bugay and A. C. Williams. Vibrational spectroscopy. In H. G. Brittain (ed.), *Physical Characterization of Pharmaceutical Solids*, Marcel Dekker, New York, 1995, Chap. 3, pp. 59–91.
6. W. P. Findlay and D. E. Bugay. Utilization of fourier transform raman spectroscopy for the study of pharmaceutical crystal forms. *J. Pharm. Biomed. Anal.* **16**:921–930 (1998).
7. C. J. Frank. Review of pharmaceutical applications of raman spectroscopy. In M. J. Pelletier (ed.), *Analytical Applications of Raman Spectroscopy*, Blackwell Science, London, 1999, Chap. 6, pp. 224–275.
8. D. E. Bugay. Solid-state nuclear magnetic resonance spectroscopy: theory and pharmaceutical applications. *Pharm. Res.* **10**:317–327 (1993).
9. D. E. Bugay. Magnetic resonance spectrometry. In H. G. Brittain (ed.), *Physical Characterization of Pharmaceutical Solids*, Marcel Dekker, New York, 1995, Chap. 4, pp. 93–125.
10. P. A. Tishmack, D. E. Bugay, and S. R. Byrn. Solid-state nuclear magnetic resonance spectroscopy—pharmaceutical applications. *J. Pharm. Sci.* **92**:441–474 (2003).
11. M. Tanaka, H. Matsui, J.-I. Mizoguchi, and S. Kashino. Optical properties, thermochromism, and crystal structures of the dimorphs of 2-iodoanilinium picrate. *Bull. Chem. Soc. Jpn.* **67**:1572–1579 (1994).
12. Y. Inouye and Y. Sakaino. Red, orange, and yellow crystals of 4,5-bis(4-methoxy phenyl)-2-(3-nitrophenyl)-1*H*-imidazole. *Acta Crystallogr.* **C56**:884–887 (2000).
13. X. He, U. J. Griesser, J. G. Stowell, T. B. Borchardt, and S. R. Byrn. Conformational color polymorphism and control of crystallization of 5-methyl-2-nitrophenyl)amino]-3-thiophenecarbonitrile. *J. Pharm. Sci.* **90**:374–388 (2001).
14. J. R. Lakowicz. *Principles of Fluorescence Spectroscopy*, 2nd ed. Kluwer/Plenum, New York, 1999.
15. H. G. Brittain. Fluorescence studies of the transformation of carbamazepine anhydrate form-III to its dihydrate phase. *J. Pharm. Sci.* **93**:375–383 (2004).
16. M. L. Cotton and R. A. Hux. Diflunisal. In K. Florey (ed.), *Analytical Profiles of Drug Substances*, Academic Press, Orlando, 1985, Chap. 15, pp. 491–526.
17. M. C. Martinez-Oharriz, C. Martin, M. M. Goni, C. Rodriguez-Espinosa, M. C. Tros de Ilarduya-Apaolaza, and M. Sanchez. Polymorphism of diflunisal: isolation and solid-state characteristics of a new crystal form. *J. Pharm. Sci.* **83**:174–177 (1994).
18. L. K. Hansen, G. L. Perlovich, and A. Bauer-Brandl. The 1:1 hydrate of diflunisal. *Acta Cryst.* **E57**:o477–o479 (2001).
19. L. K. Hansen, G. L. Perlovich, and A. Bauer-Brandl. Diflunisal-hexane (4/1). *Acta Cryst.* **E57**:o604–o606 (2001).
20. A. Bauer-Brandl, G. L. Perlovich, and L. K. Hansen. Interrelation between thermochemical and structural data of polymorphs exemplified by diflunisal. *J. Pharm. Sci.* **91**:1036–1045 (2001).
21. W. I. Cross, N. Blagden, R. J. Davey, R. G. Pritchard, M. A. Neumann, R. J. Roberts, and R. C. Rowe. A whole output strategy for polymorph screening: combining crystal structure prediction, graph set analysis, and targeted crystallization experiments in the case of diflunisal. *Cryst. Growth Des.* **3**:151–158 (2003).
22. C. A. Parker. *Photoluminescence of Solutions*, Elsevier, Amsterdam, 1968pp. 186–191.
23. J. I. Frenkel. On the transformation of light into heat in solids. *Phys. Rev.* **37**:151–158 (2003).
24. A. S. Davydov. *Theory of Molecular Excitons*, McGraw-Hill, New York, 1962.
25. D. P. Craig and S. H. Walmsley. *Excitons in Molecular Crystals*, W.A. Benjamin, New York, 1968.
26. D. P. Craig and P. C. Hobbins. The polarized spectrum of anthracene. Part I, the assignment of the intense short wavelength system. *J. Chem. Soc. London* 539–548 (1955).